[11] The NMR spectra for **1a**·**1a** and **1b**·**1b** were measured at 298 K, as the complexes are kinetically stable on the chemical shift timescale at this temperature. In contrast, it was necessary to record the NMR spectra of (+)-**2a**·(−)-**2a** and (+)-**2b**·(−)-**2b** at 263 K to achieve kinetic stability. We attempted to determine the thermodynamic stability of these aggregates by ^{1}H NMR dilution experiments in $CDCl_3$, but did not observe any changes in chemical shift upon dilution to 100 μM. Isothermal titration calorimetry yielded thermodynamic parameters for dimerization (C_6H_6/DMSO 95:5, 298 K, **1a**·**1a**: $K_a = 5550 \pm 1230\,M^{-1}$, $\Delta H = -15.7 \pm 0.9\,kJ\,mol^{-1}$).

[12] CCDC-187956 (**1a**·**1a**) and CCDC-187957 ((+)-**2b**·(−)-**2b**) contains the supplementary crystallographic data for this paper. These data can be obtained free of charge via www.ccdc.cam.ac.uk/conts/retrieving.html (or from the Cambridge Crystallographic Data Centre, 12, Union Road, Cambridge CB2 1EZ, UK; fax: (+44) 1223-336-033; or deposit@ccdc.cam.ac.uk).

[13] For a review on H-bond geometry, see: R. Taylor, O. Kennard, *Acc. Chem. Res.* **1984**, *17*, 320–326. For **1a**·**1a**, the two external amide protons are strongly H-bonded to the internal amide C=O groups with typical separations (N···O 2.937 Å, H···O 2.088 Å) and angles (N–H···O 162.0°), whereas the structural data indicates that the internal amide N–H groups may benefit from weaker interactions with the ureidyl C=O moiety (N···O 2.909 Å, H···O 2.240 Å; N-H···O 132.6°). For (+)-**2b**·(−)-**2b**, the two external amide protons H-bonded to the internal amide C=O groups have typical geometries (N···O 2.860 Å, H···O 2.014 Å; N-H···O 160.8°), whereas the internal amide protons clearly do not benefit from additional interactions (N···O 3.296 Å, H···O 2.683 Å).

[14] Selected reviews: J.-M. Lehn, *Chem. Eur. J.* **1999**, *5*, 2455–2463; P. Timmerman, D. N. Reinhoudt, *Adv. Mater.* **1999**, *11*, 71–74; S. J. Rowan, S. J. Cantrill, G. R. L. Cousins, J. K. M. Sanders, J. F. Stoddart, *Angew. Chem.* **2002**, *114*, 938–993; *Angew. Chem. Int. Ed.* **2002**, *41*, 899–952.

[15] The observed self-sorting phenomenon can be explained based on either kinetic or thermodynamic arguments. The lifetimes of the kinetically more stable dimers determined by ^{1}H EXSY NMR measurements (**1a**·**1a**: 13.6 s^{-1}; **1b**·**1b**: 6.3 s^{-1}) indicate that a fast exchange occurs, which rules out a kinetically controlled process and implies a thermodynamic preference for self-sorting in this system.

Novel Liquid-Crystalline Phases with Layerlike Organization**

Xiao Hong Cheng, Malay Kumar Das, Siegmar Diele, and Carsten Tschierske*

Investigation of the driving forces of molecular self-organization is one of the most exciting and most rapidly growing areas of chemical research. In this respect, ordered structures with liquid-crystalline (LC) properties are of special interest, because they are reversibly formed under thermodynamic equilibrium conditions and combine order and mobility on molecular, supramolecular, and macroscopic levels. The mobility enables them to respond to different external stimuli by changing their configuration, which in turn determines their importance in biological systems and technical applications.[1] In conventional LC materials rod- or disklike anisometric rigid units, which provide long-range orientational order, are connected to flexible alkyl chains, which are largely responsible for positional order and mobility. This design principle leads to the well-known nematic, smectic, and columnar LC phases.[2] A characteristic feature of such LC materials is a molecular topology in which rigid cores and flexible chains are connected in such a manner that the parallel organization of the rigid segments and the segregation of the incompatible molecular parts enhance each other.

Exciting new mesophase morphologies can be realized if rodlike (calamitic) rigid units are combined with two incompatible subunits in a competitive and nonlinear manner.[3,4] Examples are bolaamphiphilic biphenyl derivatives carrying a long lateral alkyl chain.[4] In such bolaamphiphiles, the strongest attractive forces (hydrogen bonding) act at the two termini of a rigid calamitic core. The lateral alkyl chains represent a third group of units that are incompatible with both the polar terminal diol groups[5] and the rigid biphenyl cores. As a consequence, each of these units segregates into its own subspace, and a series of unusual columnar mesophases results. They are built up by networks of cylinders, formed by ribbons of the biphenyl cores which are held together by ribbons of hydrogen-bonding networks (see Figure 1). The

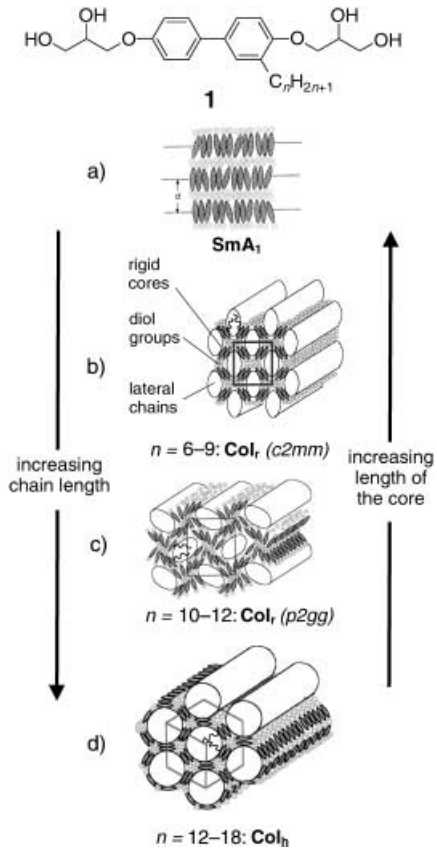

Figure 1. Molecular organization of compounds **1** in their mesophases in dependence on the molecular structure.[4]

[*] Prof. Dr. C. Tschierske, Dr. X. H. Cheng
Institute of Organic Chemistry
Martin-Luther-University Halle-Wittenberg
Kurt-Mothes-Str. 2, 06120 Halle (Germany)
Fax: (+49) 345-55-27223
E-mail: tschierske@chemie.uni-halle.de
Dr. M. K. Das, Dr. S. Diele
Institute of Physical Chemistry
Martin-Luther-University Halle-Wittenberg

[**] This work was supported by the Deutsche Forschungsgemeinschaft, the Fonds der Chemischen Industrie, and the European Commission (RTN LCDD).

  0044-8249/02/11421-4203 $ 20.00+.50/0

interior of these cylinders is filled with columns of the microsegregated fluid lateral chains. Figure 1 gives an overview of the obtained mesophase structures. First, the mesophase type depends on the length of the lateral chain, that is, their space requirement. Second, it depends on the space available for the chains within the cylinders, which is determined by the length of the bolaamphiphilic core.[4] The question arose what would happen if the ratio of the size of the nonpolar chains and the length of the bolaamphiphilic core is shifted further, so that the formation of cylinders becomes disfavored.

Here we report novel mesophases obtained with the new mesogenic block molecules **2**–**4**. They have the same fundamental structure as compounds of the type **1**, but replacement of one of the terminal 2,3-dihydroxypropoxy groups by a single OH group makes the bolaamphiphilic core shorter and reduces the number of possible hydrogen bonds. Additionally, the lateral alkyl chains are replaced by semiperfluorinated chains,[6] which require much more space than related hydrocarbon chains.[7] Moreover, the stronger segregation[8] of such fluorinated chains from the polar and rigid molecular parts (PR parts) increases the mesophase stability and thus compensates for the mesophase destabilization that results from the reduced cohesive forces between the bolaamphiphilic cores (fewer hydrogen bonds). Both structural variations lead to a dramatic change in self-organization in comparison to compounds **1**.

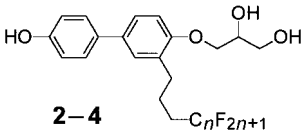

2–4

These compounds were synthesized as shown in Scheme 1.[13] The products were investigated by differential scanning calorimetry (DSC), polarized light microscopy, and X-ray diffraction of well-aligned samples. The observed mesophases and their transition temperatures are collected in Table 1.

Compound **3** has the richest polymorphism and will be discussed in more detail. Three distinct mesophases can be detected by polarized light optical microscopy (see Figure 2). The high-temperature mesophase behaves like a conventional SmA phase, characterized by a typical fan texture (Figure 2a) which can easily be aligned homeotropically. These homeotropically aligned areas are optically isotropic and appear completely dark between crossed polarizers (Figure 2b). On cooling, at 153 °C a schlieren texture appears in these regions (Figure 2e) and indicates the transition to a new optically biaxial mesophase. A characteristic feature of this schlieren texture is the absence of four-brush disclinations. This excludes an SmC-like organization in which the molecules are tilted with respect to the layer planes and

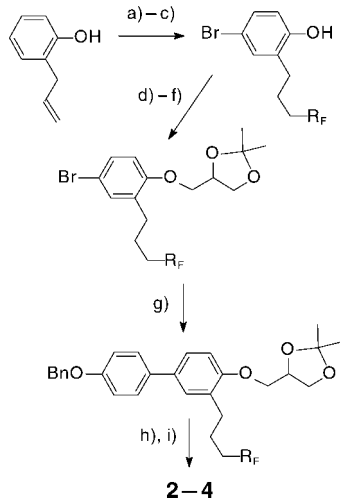

2–4

Scheme 1. Synthesis of **2**–**4**. a) R_FI, $[Pd(PPh_3)_4]$;[9] b) $LiAlH_4$, Et_2O; c) HBr, AcOH, DMSO;[10] d) $BrCH_2CH{=}CH_2$, K_2CO_3, MeCN; e) *N*-methylmorpholine *N*-oxide, cat. OsO_4, acetone, H_2O;[11] f) 2,2-dimethoxypropane, Py·TosOH; g) $(4\text{-BnO})C_6H_4B(OH)_2$, $[Pd(PPh_3)_4]$, $NaHCO_3$, glyme;[12] h) 10% HCl, EtOH; i) H_2, Pd/C, EtOAc. $R_F = C_nF_{2n+1}$ ($n = 8$, 10, 12).

which is often found in conventional LC materials below an SmA phase. In samples with a fanlike texture only a significant change in the birefringence can be observed at the phase transition. The color changes from yellow through red, violet, blue, and green to yellow again, but the fans do not break or change their shape (Figure 2d). These textural features were predicted for biaxial SmA phases (SmA_b, McMillan phase)[14] and were recently observed experimentally for such a mesophase.[15] The transition to the third mesophase at 152 °C can be seen by the transformtion of the schlieren texture into a paramorphotic mosaiclike texture (Figure 2h),[16] whereas no change is observed in the regions with fan-shaped texture. Here only the color changes, from deep yellow to red (Figure 2g). This suggests that the layer structure itself remains nearly unchanged in all three phases, whereas the order within the layers changes dramatically. This is additionally confirmed by X-ray scattering. The X-ray diffraction pattern does not change at the phase transitions between the three distinct phases. As shown in Figure 3 it is characterized by diffuse scattering in the wide-angle region,

Table 1. Transition temperatures T [°C] and corresponding enthalpy values ΔH [kJ mol^{-1}] (lower lines) of compounds **2**–**4**.[a]

Comp	*n*	Cr		Lam_A		SmA_b		SmA		IS
2	8	●	118 [0.8][b]	●		–		–	139 [6.0]	●
3	10	●	135[c] [37.2]	●	152	● [2.0][d]	153	●	156 [1.7]	●
4	12	●	154[c] [18.6]	–		(●	142)	●	188 [2.0]	●

[a] Abbreviations: Cr = crystalline solid state; Lam_A = laminated smectic A phase, see Figure 2i;[20] SmA_b = biaxial smectic A phase, see Figure 2f; SmA = smectic A phase, see Figure 2c; Iso = isotropic liquid phase. Transition temperatures and enthalpies were determined by DSC (Perkin-Elmer DSC-7, first heating scan, rate: 10 K min^{-1}) and confirmed by polarized light optical microscopy. Values in parentheses refer to monotropic (metastable) phases which were determined in the second heating scan. [b] Only partial crystallization, glassy solidification at $T_g = 18$ °C. [c] Multiple melting and Cr–Cr transitions were observed. [d] Not resolved.

  0044-8249/02/11421-4204 $ 20.00+.50/0 *Angew. Chem.* **2002**, *114*, Nr. 21

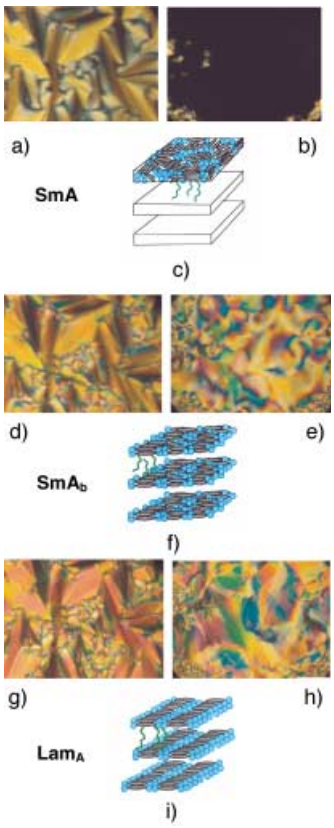

Figure 2. Textures of the mesophases of compound **3**, as observed between crossed polarizers, and suggested models of the organization of the molecules in the distinct mesophases. a) Fan-shaped texture of the SmA phase at 155 °C. b) Homeotropically aligned SmA phase at 155 °C. c) Organization of the molecules in the SmA phase. d) Fan-shaped texture of the SmA_b phase at 152.5 °C. e) Schlieren texture of the SmA_b phase at 152.5 °C. f) Organization of the molecules in the SmA_b phase. g) Fan-shaped texture of the Lam_A phase at 140 °C. h) Paramorphotic mosaic texture at 145 °C. i) Organization of the molecules in the Lam_A phase.[20]

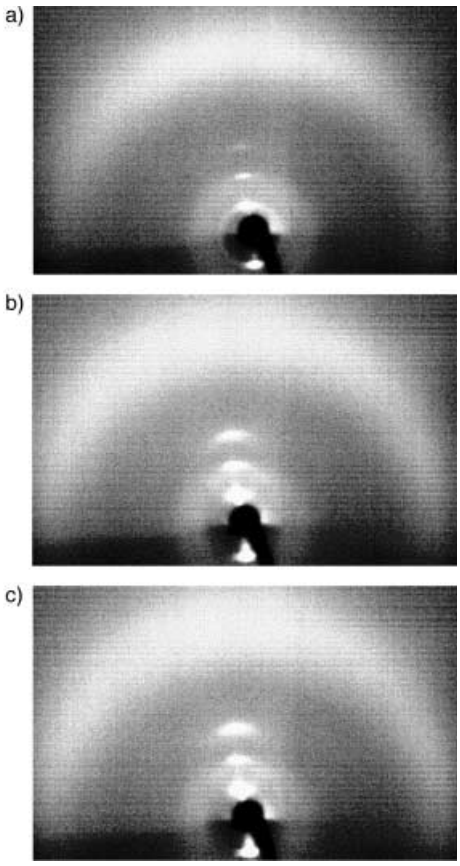

Figure 3. X-ray diffraction pattern of an aligned sample of compound **3** a) in the SmA phase at 155 °C, b) in the SmA_b phase at 152.5 °C, and c) in the Lam_A phase at 144 °C.

which indicates the fluid state of this mesophase. Additionally, the small-angle region contains three sharp equidistant reflections that indicate the presence of a well-defined layer structure. The layer thickness is $d = 3.41$ nm at $T = 137$ °C and is nearly temperature independent. No change of the layer thickness can be detected at the phase transitions. However, the layer spacing significantly increases with elongation of the lateral alkyl chain (**2**: $d = 3.0$ nm, **4**: $d = 3.8$ nm). The most remarkable feature of the X-ray diffraction pattern of well-oriented samples shown in Figure 3[17] is that the diffuse wide-angle scattering forms a ring ($D = 0.49$ nm) with a maximum intensity at the meridian, that is, in the same direction as the layer reflection. This diffraction pattern is completely different from those of conventional smectic A phases, for which crescentlike halos are located perpendicular to the direction of the layer reflections.

The microscopic observations together with the peculiarities of the X-ray pattern led to the models of the mesophase structures shown in Figure 2c, f, and i. Accordingly, the layer structure should be the result of segregation of the nonpolar lateral chains from the bolaamphiphilic PR parts (biphenyl units and terminal diol groups). The layers are formed parallel to the molecular long axes, and this means that, in contrast to all conventional smectic phases, the calamitic biphenyl cores are organized parallel to the layer planes. The PR layers are separated by the nonpolar layers of the lateral chains, which are strongly disordered (liquidlike). This special organization should be provided 1) by the unique topology of connection of the nonpolar chains in a lateral position at the rodlike cores, 2) by the parallel alignment of the biphenyl cores, and 3) by the cohesive hydrogen bonds at the termini of the biphenyl cores, which stabilize the PR layers. The experimentally determined layer distance requires that the thickness of the PR sublayers correspond on average to about three parallel aligned biphenyl cores. According to X-ray scattering and optical investigations, the layer structure is maintained in all three mesophases. Therefore, the phase transitions should result from a reorganization of the biphenyl cores within the PR layers.

Let us at first consider the biaxial smectic phase SmA_b shown in Figure 2f. Here, the biphenyl cores should adopt long-range orientational order within the PR sublayers, and the individual layers are orientationally correlated with each other, so that optical biaxiality of the bulk sample results. Hence, this biaxial smectic phase is built up by a regular sequence of thin layers of the ordered PR cores, separated by the layers of the lateral chains. Since only orientational order of the PR cores exists within the layers, this phase can be regarded as a nematic phase which is laminated parallel to the long axis of the calamitic molecules.

  0044-8249/02/11421-4205 $ 20.00+.50/0

At the transition to the high-temperature mesophase SmA either the long-range parallel alignment of the rigid cores within the PR layers or the orientational correlation between adjacent layers may be lost. It is, however, most likely that the two processes occur simultaneously. This means that the formation of a long-range orientational order within the individual layers at the transition from the uniaxial SmA to the biaxial SmA_b phase is accompanied by the formation of a long-range orientational correlation between adjacent layers. Hence, the phase structure of this SmA phase is related to those of conventional SmA phases, with the difference that in this new phase the biphenyl cores should be aligned on average parallel to the layer planes (see Figure 2c).[18]

The transition from the SmA_b phase to the low-temperature phase is characterized by a reduction in the fluidity, as indicated by the transition from a schlieren texture to a paramorphotic mosaiclike texture. This means that additional order should occur at this phase transition. In analogy to the phase sequence Iso-N-SmA, which is often observed in conventional LC systems on decreasing the temperature, it can be assumed that in the low-temperature mesophase of **3** the bolaamphiphilic cores adopt a positional order within the PR sublayers. This results from the segregation of the hydrogen-bonding networks from the aromatic cores which leads to a smecticlike organization within these sublayers (see Figure 2i). Hence, microsegregation occurs in two distinct directions: Segregation of the nonpolar chains from the PR cores leads to the "bulk" layer structure, and segregation of polar and aromatic subunits within the PR layers gives rise to an additional periodicity within these sublayers which occurs parallel to the layer planes. As the wide-angle scattering remains diffuse in all three mesophases, no additional order between the aromatic cores (e.g., SmB-like) or within the sublayers of the lateral chains should occur in this low-temperature mesophase. In other words, this mesophase can be regarded as a fluid smectic phase which is laminated parallel to the molecular long axes by the fluid layers of the lateral chains. Because we have no particular indication for a tilted arrangement of the molecules within these quasi-2D smectic sublayers[19] the simplest possibility for a laminated SmA structure (Lam_A)[20] is suggested for this mesophase (Figure 2i). Surprisingly, however, the additional repeat distance within the PR sublayers, which is expected to occur perpendicular to the layer reflection at the equator of the two-dimensional X-ray pattern, cannot be found in the X-ray diffraction pattern. This could be explained by assuming that the electron-density modulation within the 2D smectic sublayers is low;[21] hence, the intensity of the corresponding reflections is very low. Additionally, there is no positional correlation between adjacent layers, and this means that there is only an orientational correlation of adjacent layers, but the individual layers can still slide with respect to each other. This phase structure has some similarities to the sliding columnar[22] and lamellar columnar mesophases.[23]

These results show that the competitive combination of microsegregation and rigidity is an appropriate way to obtain exciting new mesophase morphologies that are quite distinct from conventional mesophases. The individual sheets of these lamellar arrangements can be regarded as quasi-2D analogues of the classical 3D mesophases. Hence, it could be expected that a diversity of different higher-order structures related to those known from conventional smectic phases could also be obtained within the layers of these laminated mesophases. Additional new mesophases could be expected at the transition between the columnar phases of compounds **1** and the smectic phases of **2**–**4**, and as a result of the positional correlation between adjacent layers of the laminated smectic phases, and this would lead to numerous novel mesophases with two- and three-dimensional organization.[24]

Received: June 24, 2002 [Z19590]

[1] J.-M. Lehn, *Supramolecular Chemistry*, VCH, Weinheim, **1995**.

[2] D. Demus, J. Goodby, G. W. Gray, H. W. Spiess, V. Vill, *Handbook of Liquid Crystals*, Wiley-VCH, Weinheim, **1998**.

[3] J. A. Schröter, C. Tschierske, M. Wittenberg, J. H. Wendorff, *J. Am. Chem. Soc.* **1998**, *120*, 10669.

[4] M. Kölbel, T. Beyersdorff, X. H. Cheng, C. Tschierske, J. Kain, S. Diele, *J. Am. Chem. Soc.* **2001**, *123*, 6809.

[5] C. Tschierske, *Prog. Polym. Sci.* **1996**, *21*, 775.

[6] Selected examples of LC materials with fluorinated chains: a) F. Guittard, E. Taffin de Givenchy, S. Geribaldi, A. Cambon, *J. Fluorine Chem.* **1999**, *100*, 85; b) H. T. Nguyen, G. Sigaud, M. F. Achard, F. Hardouin, R. J. Twieg, K. Betterton, *Liq. Cryst.* **1991**, *10*, 389; c) T. Doi, Y. Sakurai, A. Tamatani, S. Takenaka, S. Kusabashi, Y. Nishihata, H. Terauchi, *J. Mater. Chem.* **1991**, *1*, 169; d) S. V. Arehart, C. Pugh, *J. Am. Chem. Soc.* **1997**, *119*, 3027; e) S. Pensec, F.-G. Tournilhac, P. Bassoul, C. Durliat, *J. Phys. Chem.* **1998**, *102*, 52; f) S. Diele, D. Lose, H. Kruth, G. Pelzl, F. Guittard, A. Cambon, *Liq. Cryst.* **1996**, *21*, 603; g) U. Dahn, C. Erdelen, H. Ringsdorf, R. Festag, J. H. Wendorff, P. A. Heiney, N. C. Maliszewskyj, *Liq. Cryst.* **1995**, *19*, 759; h) V. Percec, G. Johansson, G. Ungar, J. Zhou, *J. Am. Chem. Soc.* **1996**, *118*, 9855; i) A. Pegenau, X.-H. Cheng, C. Tschierske, P. Göring, S. Diele, *New. J. Chem.* **1999**, *23*, 465; k) M.-A. Guillevic, D.-W. Bruce, *Liq. Cryst.* **2000**, *27*, 153.

[7] a) X. H. Cheng, C. Tschierske, P. Göring, S. Diele, *Angew. Chem.* **2000**, *112*, 605; *Angew. Chem. Int. Ed.* **2000**, *39*, 592; b) X. H. Cheng, M. K. Das, S. Diele, C. Tschierske, *Langmuir* **2002**, *18*, 6521.

[8] C. Tschierske, *J. Mater. Chem.* **2002**, *11*, 2647.

[9] Q.-Y Chen, Z. Y. Yang, C.-X. Zhao, Z. M. Qiu, *J. Chem. Soc. Perkin Trans. 1* **1988**, 563.

[10] G. Majetch, R. Hicks, S. Reister, *J. Org. Chem.* **1997**, *62*, 4321.

[11] V. Van Rheenen, D. Y. Cha, W. M. Hartley, *Org. Synth.* **1979**, 58, 43.

[12] a) N. Miyaura, T. Yanagi, A. Suzuki, *Synth. Commun.* **1981**, *11*, 513; b) M. Hird, G. W. Gray, K. J. Toyne, *Mol. Cryst. Liq. Cryst.* **1991**, *206*, 187.

[13] All analytical data are in accordance with the proposed structures; for example, **3**: ^{1}H NMR (400 MHz; [D$_6$]DMSO): $\delta = 9.36$ (s, 1H, OH), 7.33 (d, ^3J(H,H) = 8.6 Hz, 2H, ArH), 7.28 (m, 2H, ArH), 6.91 (d, ^3J(H,H) = 8.4 Hz, 1H, ArH), 6.77 (d, ^3J(H,H) = 8.6 Hz, 2H, ArH), 4.84 (br s, 1H, CHO*H*), 4.58 (m, 1H, CH_2O*H*), 3.76–3.49 (m, 3H, ArCH_2OC*H*)), 3.46 (m, 2H, CH_2OH), 2.60 (t, 2H, ^3J(H,H) = 7.2 Hz, CH_2Ar), 2.08 (2H, CH_2CF_2), 1.75 (m, 2H, CH_2); ^{13}C NMR (100 MHz; [D$_6$]DMSO): $\delta = 156.6$, 155.6, 132.7, 131.1 129.4, 127.4, 127.3, 125.1, 115.6, 112.1, 70.0, 69.5, 62.7, 29.8, 20.1; ^{19}F NMR (188 MHz; [D$_6$]DMSO): $\delta = -82.46$ (3F, CF_3), -114.40 (2F, CH_2CF_2), -122.74 (m, 12F, CF_2), -123.91 (2F, $CF_2CF_2CF_3$), -127.32 (2F, CF_2CF_3); elemental analysis (%) calcd for $C_{28}H_{21}O_4Si_{21}$: C 40.99, H 2.58; found: C 40.83, H 2.99.

[14] H. R. Brand, P. E. Cladis, H. Pleiner, *Macromolecules* **1992**, *25*, 7223.

[15] T. Hegmann, J. Kain, G. Pelzl, S. Diele, C. Tschierske, *Angew. Chem.* **2001**, *113*, 911; *Angew. Chem. Int. Ed.* **2001**, *40*, 887.

[16] The texture of the Lam_A phase of compound **2** which occurs directly from the isotropic liquid state is not a paramorphotic texture and therefore typical mosaic and spherulitic textures can be observed.

[17] The alignment is obtained by spreading the samples on a glass substrate, without applying external electric or magnetic fields.

  0044-8249/02/11421-4206 $ 20.00+.50/0

[18] A related phase structure should be present in the SmA phases of a TTF derivative with four branched lateral chains (R. A. Bissell, N. Boden, R. J. Bushby, C. W. G. Fishwick, E. Holland, B. Movaghar, G. Ungar, *Chem. Commun.* **1998**, 113.) and was suggested for 1,4,5,8-tetraalkyl-substituted derivatives of anthracene and anthraquinone (S. Norvez, F. G. Tournilhac, P. Bassoul, P. Hersonn, *Chem. Mater.* **2001**, *13*, 2552).

[19] In this case, which would correspond to laminated SmC or SmC_A structures, the aromatic cores would be tilted with respect to the direction of the periodicity within the aromatic sublayers, but parallel to the layer planes of the bulk organization.

[20] To distinguish such phases from conventional smectic phases, in which the calamitic molecules are arranged perpendicular to or tilted with respect to the layer planes, it is proposed to designate such phases as laminated mesophases (Lam), whereby a subscript designates the organization within the ordered sublayers (Lam_A = laminated SmA phase, see Figure 2i). In principle, the SmA_b and SmA phases of **2**–**4** can alternatively be described as a laminated nematic phase (Lam_N) and laminated isotropic phases (Lam_{Iso}), respectively, but the phase symmetry of these phases is the same as in conventional SmA_b and SmA phases, so that this-well established nomenclature should still be used in these cases.

[21] a) F. Hardouin, H. T. Nguyen, M. F. Achard, A. M. Levelut, *J. Phys. Lett.* **1982**, *3*, L-327; b) B. I. Ostrovskii, *Liq. Cryst.* **1993**, *14*, 131.

[22] T. C. Lubensky, C. S. O'Hern in *Slow Dynamics in Complex Systems: Eighth Tohwa University International Symposium*, (Ed.: M. Tokuyama, I. Oppenheim), The American Institute of Physics, Woodbury, NY, **1999**, p. 105.

[23] a) A. M. Levelut, M. Ghedini, R. Bartolino, F. P. Nicoletta, F. Rustichelli, *J. Phys. (Paris)* **1989**, *50*, 113; b) R. Ziessel, L. Douce, A. El-ghayoury, A. Harriman, A. Skoulios, *Angew. Chem.* **2000**, *112*, 1549; *Angew. Chem. Int. Ed.* **2000**, *39*, 1489.

[24] A crystalline SmG-like organization of aromatic cores was proposed for the aromatic layers of 1,4,5,8-tetraalkyl-substituted derivatives of anthracene and anthraquinone.[18b]

A Practical and Highly Active Ruthenium-Based Catalyst that Effects the Cross Metathesis of Acrylonitrile**

Jennifer A. Love, John P. Morgan, Tina M. Trnka, and Robert H. Grubbs*

The N-heterocyclic carbene-coordinated ruthenium benzylidene complex $[(H_2IMes)(PCy_3)(Cl)_2Ru{=}CHPh]$ (**1**) is a highly active catalyst for a wide variety of olefin-metathesis reactions,[1] including those with sterically demanding[2] and electron-deficient olefins (Scheme 1).[3] In spite of recent advances, there are several processes that remain challenging,

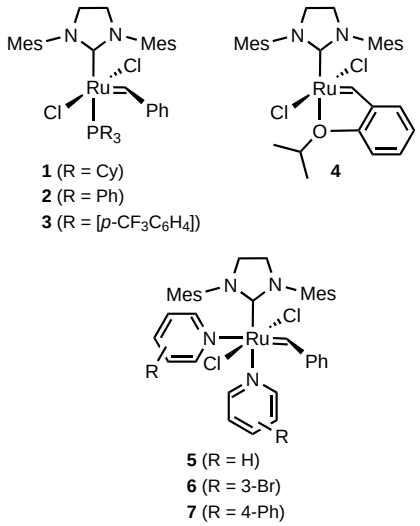

Scheme 1. Ruthenium-based olefin metathesis catalysts. Mes = 2,4,6-trimethylphenyl.

such as olefin cross metathesis (CM) with directly functionalized olefins.[4] For example, acrylonitrile CM has only been successful with Schrock's arylimido molybdenum alkylidene catalyst[5] and the ether-tethered ruthenium alkylidene derivative $[(H_2IMes)(Cl)_2Ru{=}CH(o\text{-}i\text{PrOC}_6H_4)]$ (**4**).[6,7] Phosphane-ligated ruthenium catalysts have given poor results for this transformation,[3a,5c,6c,8,9] except for one report of efficient CM between purified acrylonitrile and 1-decene mediated by **1**.[10] We have determined that dissociation rates of ligands are related to catalyst efficiency during CM with acrylonitrile. On this basis, we have developed a new, highly efficient ruthenium complex to perform acrylonitrile CM with unpurified acrylonitrile; this catalyst is the *fastest initiator* of any ruthenium-based catalyst reported to date.[11]

Previous studies have shown that precatalysts of the type $[L_2X_2Ru{=}CHR]$ initiate by dissociating one L-type ligand before entering the catalytic cycle (Scheme 2);[12] in complexes **1**–**3**, L is a phosphane (PR_3), and in complex **4**, L is a tethered ether ligand (*i*PrO). Importantly, complexes **1**–**4** all provide the *same* propagating species (**A** and **B**) after a *single* turnover.[13] If either **A** or **B** is trapped by L, dissociation of L must occur before catalysis can continue. The relative affinity of **A** and/or **B** for the olefin in preference to L (i.e., favoring propagation) controls how long these species remain in the catalytic cycle. Consequently, the differences in activity between catalysts **1**–**4** depend on their rates of initiation and rebinding of L, both of which can be tuned by the nature of L.[12b,14–16]

Complexes **1**–**4** are all active for a variety of metathesis processes, such as CM, ring-closing metathesis (RCM), and ring-opening-metathesis polymerization (ROMP). However, the situation involving acrylonitrile CM is more complex; CM between acrylonitrile and allylbenzene proceeds efficiently with **4** (68% yield) but not with **1**–**3** (21%, 35%, and 36% yields, respectively; Table 1).[17] Clearly, this difference cannot simply be an issue of precatalyst initiation; **2** and **4** have roughly the same initiation rates and initiation is faster with **3** than **1**, **2**, or **4** Table 2. The difference is also not a result of

[*] Prof. R. H. Grubbs, Dr. J. A. Love, J. P. Morgan, T. M. Trnka
Arnold and Mabel Beckman Laboratory of Chemical Synthesis
Division of Chemistry and Chemical Engineering
California Institute of Technology
Pasadena, CA 91125 (USA)
Fax: (+1) 626-564-9297
E-mail: rhg@its.caltech.edu

[**] This work was funded by the National Science Foundation. J.A.L. acknowledges the National Institutes of Health for a postdoctoral fellowship, and T.M.T. acknowledges the Department of Defense for a NDSEG graduate fellowship.

Supporting information for this article is available on the WWW under http://www.angewandte.org or from the author.